

Nanocrystal bilayer for tandem catalysis

Yusuke Yamada^{1†}, Chia-Kuang Tsung^{1,2†}, Wenyu Huang^{1,2}, Ziyang Huo¹, Susan E. Habas^{1,2}, Tetsuro Soejima¹, Cesar E Aliaga², Gabor A. Somorjai^{1,2} and Peidong Yang^{1,2*}

Supported catalysts are widely used in industry and can be optimized by tuning the composition and interface of the metal nanoparticles and oxide supports. Rational design of metal–metal oxide interfaces in nanostructured catalysts is critical to achieve better reaction activities and selectivities. We introduce here a new class of nanocrystal tandem catalysts that have multiple metal–metal oxide interfaces for the catalysis of sequential reactions. We utilized a nanocrystal bilayer structure formed by assembling platinum and cerium oxide nanocube monolayers of less than 10 nm on a silica substrate. The two distinct metal–metal oxide interfaces, CeO₂–Pt and Pt–SiO₂, can be used to catalyse two distinct sequential reactions. The CeO₂–Pt interface catalysed methanol decomposition to produce CO and H₂, which were subsequently used for ethylene hydroformylation catalysed by the nearby Pt–SiO₂ interface. Consequently, propanal was produced selectively from methanol and ethylene on the nanocrystal bilayer tandem catalyst. This new concept of nanocrystal tandem catalysis represents a powerful approach towards designing high-performance, multifunctional nanostructured catalysts.

High-performance catalysts are central to the development of new-generation energy conversion and storage technologies^{1,2}. Although industrial catalysts can be optimized empirically by tuning the elemental composition, changing the supports or altering preparation conditions to achieve greater activity and selectivity, these conventional catalysts are typically not uniform in composition and/or surface structure at the nano- to microscale. To improve significantly our capability of designing better catalysts, new concepts for the rational design and assembly of metal–metal oxide interfaces are desirable. Metal nanocrystals with well-controlled shape and size are interesting materials for catalyst design, from both electronic structure and surface structure aspects^{3–5}. From the electronic structure aspect, small metal nanoclusters have size-dependent electronic states, which make them fundamentally different from the bulk. From the surface structure aspect, the shaped nanocrystals have surfaces with well-defined atomic arrangements. In recent decades surface-science studies have demonstrated clearly that the atomic arrangement on the crystal surface can affect catalytic phenomena in terms of activity, selectivity and durability.

The application of shape- and size-controlled metal oxide nanocrystals as catalyst supports has even greater potential for innovative catalyst design^{6,7}. It is well-known that catalysis can be modulated by using different metal oxide supports, or metal oxide supports with different crystal surfaces⁸. For example, platinum-loaded molybdenum oxide and silica catalysts show similar activation energies for ethylene hydrogenation⁹. However, the activation energy for ethane hydrogenolysis over platinum–silica was lower than that over platinum–molybdenum oxide¹⁰. It is believed that the metal oxides not only work as supports, but also function as electronic modulators, in addition to contributing spillover and adsorption sites. Precise selection and control of metal–oxide interfaces could lead to better activity and selectivity for a desired reaction¹¹.

The integration of many types of metal–metal oxide interfaces on the surface of a single active metal nanocrystal could, in principle, yield a novel tandem catalyst for multistep reactions. The catalytic

activity and selectivity of such a tandem catalyst can be optimized by establishing suitable metal–metal oxide interfaces for each reaction step. However, it is almost impossible to control the composition of multiple interfaces on an atomic level using traditional catalyst synthesis. Integrating binary nanocrystals to form highly ordered superlattices is a new way to form multiple interfaces with new functionalities^{12,13}. We utilized a nanocrystal bilayer structure formed by assembling Pt and CeO₂ nanocube monolayers of less than 10 nm on a silica substrate. The two distinct metal–metal oxide interfaces in the catalyst, CeO₂–Pt and Pt–SiO₂, were used to catalyse two separate and sequential reactions. The CeO₂–Pt interface catalysed methanol decomposition to produce CO and H₂, which were subsequently used for ethylene hydroformylation catalysed by the nearby Pt–SiO₂ interface. Consequently, propanal was produced selectively on this nanocrystal bilayer tandem catalyst.

The cubic shape of nanocrystals is ideal for assembling metal–metal oxide interfaces with a large contact area. Figure 1 shows our tactic to achieve the ‘tandem’ bilayer structure with nanocubes of metal and metal oxide. First, a two-dimensional metal (Pt) nanocube array was assembled onto a flat metal oxide substrate (SiO₂) by using the Langmuir–Blodgett (LB) method to make the first metal–metal oxide interface. The second metal oxide (CeO₂) nanocube LB array was then assembled on top of the metal nanocube monolayer, which provided the second metal–metal oxide interface. The capping agents of the nanocrystals were removed by ultraviolet/ozone treatment to form clean metal–metal oxide interfaces¹⁴. After removal of the capping agent, the vertical clefts between the nanocrystals ensured access to both catalytic interfaces and provided a high surface area in the close-packed array.

Olefin hydroformylation is an important reaction for the production of aldehydes from olefins, CO and H₂ (ref. 15). Usually, the reaction is carried out with homogeneous catalysts, such as Rh complexes. The disadvantages of this process include the use of toxic CO and explosive H₂ gas, and typically it employs high-pressure conditions and purification processes. Therefore, it would

¹Department of Chemistry, University of California, Berkeley, Berkeley, California 94720, USA, ²Materials Sciences Division, Lawrence Berkeley National Laboratory, 1 Cyclotron Road, Berkeley, California 94720, USA; [†]Present addresses: Department of Material and Life Science, Graduate School of Engineering, Osaka University 2-1 Yamada-oka, Suita, Osaka 565-0871 (Y.Y.); Department of Chemistry, Merkert Chemistry Center, Boston College, 2609 Beacon Street, Chestnut Hill, Massachusetts 02467, USA (C.T.). *e-mail: p_yang@berkeley.edu

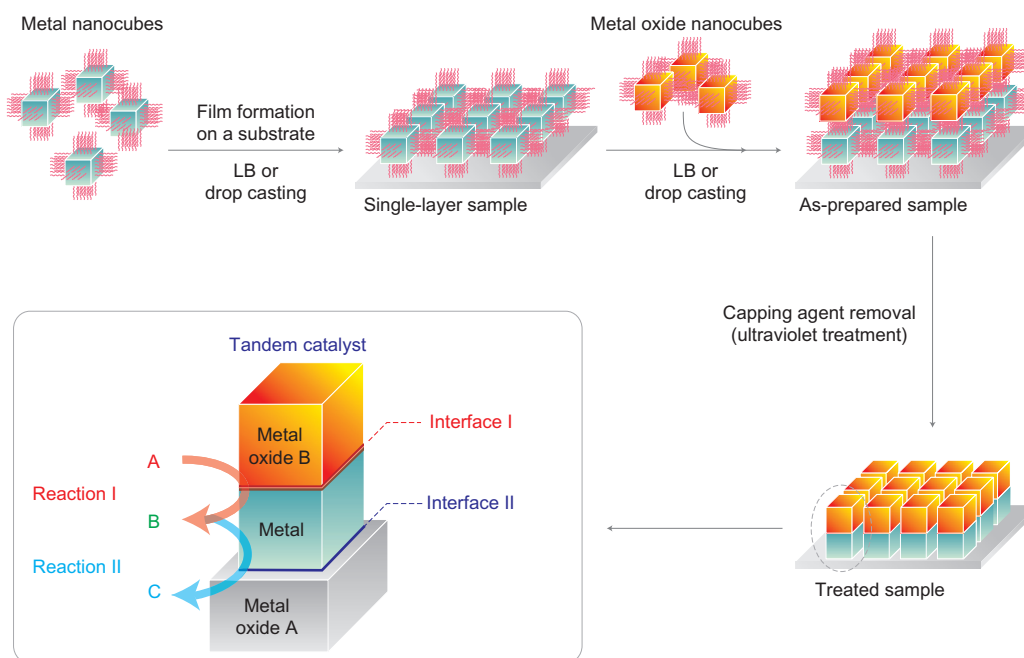


Figure 1 | Assembly process for the preparation of a nanocrystal bilayer ‘tandem catalyst’. Single layers of metal nanocubes and metal oxide cubes were deposited sequentially. Capping agents of nanoparticles were removed by ultraviolet treatment.

be advantageous to carry out olefin hydroformylation through heterogeneous catalysis with CO and H₂ produced *in situ* from the decomposition of a benign chemical, such as methanol. It is known that Pt loaded on to CeO₂ shows high activity towards methanol decomposition to provide CO and H₂ (refs 16,17). In addition, Naito and Tanimoto reported that Pt-loaded SiO₂ catalysed propene hydroformylation and produced aldehydes with a high conversion rate. However, the selectivity for this reaction was poor¹⁸. Here, we demonstrate that our nanocrystal bilayer, made of a CeO₂ nanocube monolayer and a Pt nanocube monolayer on a SiO₂ substrate, effectively catalyses ethylene hydroformylation with methanol to produce propanal selectively.

Results and discussions

Preparation of tandem catalyst. Pt and CeO₂ nanocubes with edge lengths of 6–8 nm were prepared by literature methods with minor modifications^{19,20}. A monolayer of Pt nanocubes was prepared by the LB method, and then transferred onto a silicon wafer substrate with a native oxide layer on the surface. The original capping agent on the Pt nanocubes, tetradecyltrimethylammonium bromide (TTAB), was exchanged for oleylamine to facilitate the LB assembly and deposition. A high-resolution transmission electron microscopy (HRTEM) image of a single Pt nanocube and low-magnification TEM image of a Pt LB film are shown in Fig. 2a. The Pt nanocubes were single, crystalline and enclosed by six (100) facets. The domain size of the monolayer film was over one micron by one micron, and the total coverage of the film was more than 80%. The gaps between the nanocrystals were about 2–3 nm, sufficient for the diffusion of small molecules. The CeO₂ nanocube monolayer film capped with oleic acid was prepared by either drop casting or the LB method. Figure 2b shows a film prepared by drop casting. The gaps between the nanocrystals were 4–5 nm, which is close to the thickness of the oleic acid bilayer. The drop-cast CeO₂ film showed long-range ordering. For catalytic samples, the CeO₂ film was prepared by the LB method to give a large film area. The double-layered film was obtained by depositing a CeO₂ film onto a Pt film. A TEM image of a large area of bilayered film of CeO₂ on Pt is shown in Fig. 2c. Although the CeO₂ nanocrystals above the

Pt nanocrystals cannot be observed clearly over most of the area because of their lower contrast, the CeO₂ nanocrystals are visible at some defect areas on the Pt film (Fig. 3a). The presence of CeO₂ nanocubes on the Pt nanocube film was confirmed by HRTEM and by performing an energy dispersive X-ray (EDX) spectroscopy line-scan, as shown in Fig. 3b,c. The Pt and CeO₂ lattice was observed on the bilayer film by HRTEM (Fig. 3b). The EDX line-scan over the defect area of the bilayer film (Fig. 3c) shows the intensity change of Pt and Ce along the line on the film where the Pt film is discontinuous. The Pt intensity decreased across the gap between Pt nanocrystals, but the Ce intensity was nearly constant.

To facilitate interface formation between the SiO₂, Pt and CeO₂ layers, the various capping agents, oleylamine on Pt and oleic acid on CeO₂, need to be removed. Although CeO₂ crystals are stable under high-temperature treatment to remove the capping agent, Pt nanocubes are not stable under such conditions. When Pt nanocrystal-loaded samples were heated at 250 °C in air, the shape of the Pt nanocrystals was lost. Thus, we applied a room-temperature ultraviolet irradiation process to remove the surface-capping agents. Previously, it was found that ultraviolet/ozone treatment is effective in removing organic capping agents from Pt nanoparticles¹⁸. Here, removal of the capping agent was monitored by sum frequency generation vibrational spectroscopy, as shown in Supplementary Fig. S1. Before the ultraviolet/ozone treatment, three peaks were observed and assigned to symmetric CH₂ (2,853 cm⁻¹), symmetric CH₃ (2,879 cm⁻¹) and asymmetric CH₂ (2,929 cm⁻¹) stretches. After treatment, the intensity of the peaks decreased significantly. TEM observations of the sample before and after the ultraviolet/ozone treatment indicated that the crystal shapes remained unchanged. Commonly, oxidation of CO is employed to examine the interaction between Pt and metal oxides because the activation energy of Pt loaded onto a metal oxide is highly dependent on the nature of the metal oxide support^{21–23}. The strong Pt–metal oxide interaction decreased electron donation from Pt to adsorbed CO, weakening the CO bond. As a result, the interaction between Pt and the metal oxide increased the activation energy for CO oxidation. Arrhenius plots for the CO oxidation over our CeO₂–Pt bilayers on SiO₂ substrates before and after

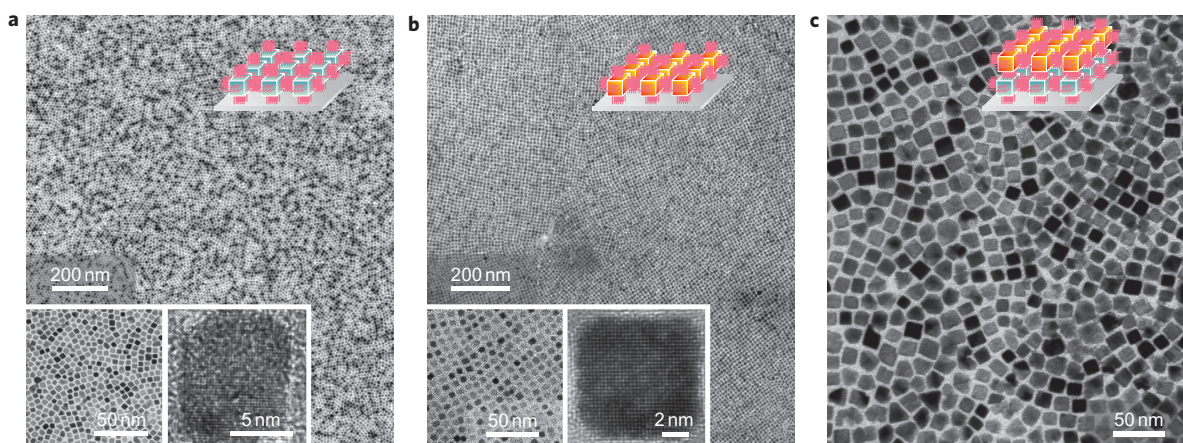


Figure 2 | Monolayer films of Pt nanocubes and CeO₂ nanocubes and a bilayer film of CeO₂-Pt nanocubes observed by TEM. a, Pt film prepared by the LB technique. **b**, CeO₂ nanocube assembly prepared by drop casting. **c**, CeO₂ nanocube monolayer on a Pt monolayer. The inset figures are the TEM images of higher magnification (left) and HRTEM images of a single nanocrystal (right).

ultraviolet/ozone treatment are shown in Supplementary Fig. S2. The as-prepared bilayers showed an apparent activation energy of 19.7 kcal mol⁻¹, which is comparable to the reported value for Pt nanocubes²². The ultraviolet/ozone-treated samples showed an apparent activation energy of 30.1 kcal mol⁻¹. The increase in activation energy indicates the formation of two metal-metal oxide interfaces of CeO₂-Pt and Pt-SiO₂ following capping-agent removal.

Ethylene hydroformylation of MeOH over a tandem catalyst. The assembly of CeO₂-Pt-SiO₂ bilayers with two different metal-metal oxide interfaces is an ideal catalyst design for olefin hydroformylation with CO and H₂ formed *in situ* by the decomposition of MeOH. It was reported previously that Pt-CeO₂ can catalyse selectively the decomposition of MeOH to give CO and H₂, and that Pt-SiO₂ catalyses olefin hydroformylation. Prior to examining the two-step tandem reaction, control experiments were performed to monitor each step over each interface individually: MeOH decomposition over the Pt-CeO₂ interface and, separately, ethylene hydroformylation with CO and H₂ gas input over the Pt-SiO₂ interface. The decomposition of MeOH over the Pt-CeO₂ interface was examined at 190 °C over a Pt-CeO₂-SiO₂ catalyst that contained only the Pt-CeO₂ metal-oxide interface. The as-prepared catalyst showed no catalytic activity for the reaction because of the lack of clean metal-metal oxide interfaces (Supplementary Fig. S3). After ultraviolet/ozone treatment, the Pt-CeO₂-SiO₂ tandem catalyst showed MeOH-decomposition activity (Fig. 4a). The concentration of formed H₂ and decomposed MeOH in the batch reactor changed in proportion to the reaction time and the ratio of formed H₂ to decomposed MeOH was 1:2, which confirms the formation of H₂ and CO. The turnover frequency (TOF) in terms of H₂ was 1.8 × 10⁻³ s⁻¹ per Pt atom. Separately, ethylene hydroformylation with CO and H₂ gas was carried out over the Pt-SiO₂ catalyst, also at 190 °C. Figure 4b shows the concentration change of propanal and MeOH in a batch reactor as a function of the reaction time. The propanal formation was observed clearly. The production of MeOH was caused by hydrogenation of CO, as confirmed by CO hydrogenation with only CO and H₂ without ethylene (Supplementary Fig. S4). The TOF in terms of MeOH was 5.8 × 10⁻² s⁻¹ per Pt atom and the TOF in terms of propanal was 2.7 × 10⁻³ s⁻¹ per Pt atom. On a bare Pt surface, the formation of MeOH by CO hydrogenation is much faster than that of propanal by hydroformylation.

Figure 5a shows time-dependent propanal formation from ethylene hydroformylation with *in situ* MeOH decomposition

over the CeO₂-Pt-SiO₂ tandem catalyst at 190 °C. The as-prepared sample produced a negligible amount of propanal even after longer reaction times (Supplementary Fig. S3). However, the formation of propanal was observed clearly over the ultraviolet/ozone-treated catalyst, as shown in Fig. 5a. This propanal formation was confirmed further by mass spectroscopy and quantified by gas chromatography (Supplementary Fig. S5). The formation of by-products such as propanol or ethane was less than the detection limit (<0.01 vol%). The maximum propanal concentration in the reaction effluent was 0.18%, at which the product selectivity towards propanal was more than 94%. This is quite surprising because simple ethylene hydrogenation, a competitive reaction of hydroformylation, is much faster on conventional Pt catalysts. The same reaction over the Pt-CeO₂-SiO₂ catalyst, which does not contain suitable interfaces for the reaction, was also performed as a control experiment. No formation of propanal was observed.

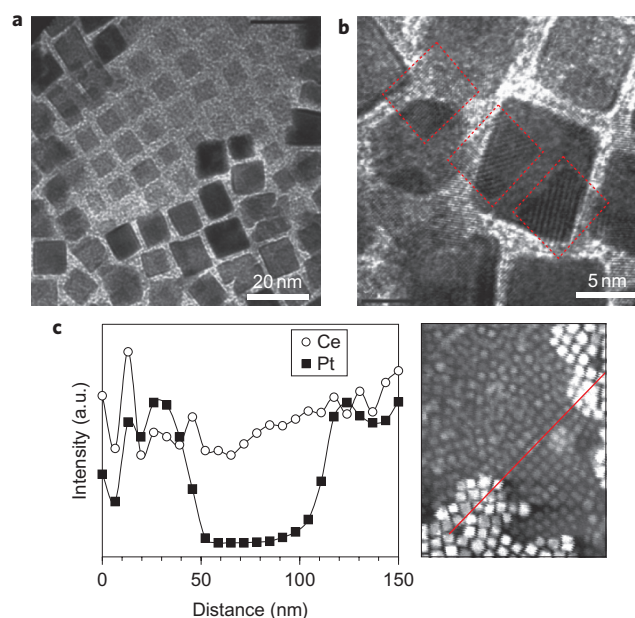


Figure 3 | Nanocrystal bilayers observed by HRTEM and EDX. a, TEM image of a defective area of a bilayer film. **b**, HRTEM image showing the overlapping CeO₂-Pt nanocubes. **c**, EDX line profile at the defective area of a bilayer film. The line profile was collected along the red trace in the image. a.u. = arbitrary units.

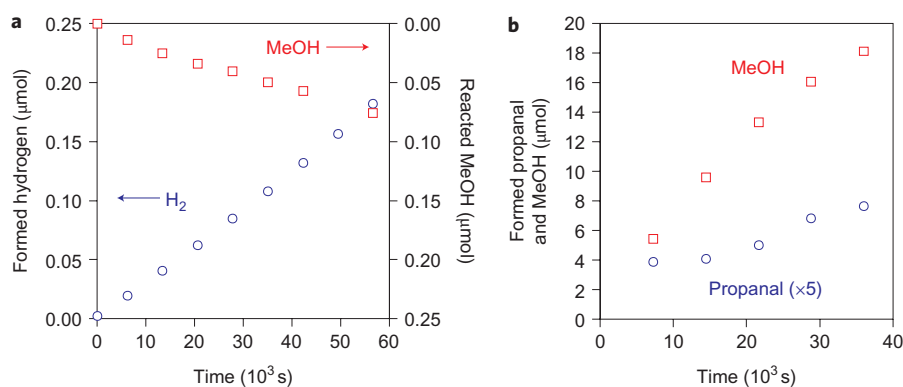


Figure 4 | MeOH decomposition over Pt–CeO₂ and conventional hydroformylation over Pt–SiO₂. **a**, H₂ produced as a function of reaction time over Pt on CeO₂ at 190 °C by catalytic thermal decomposition of MeOH. Open circles = formed H₂; open squares = decomposed MeOH. **b**, Propanal and MeOH produced as a function of reaction time over a Pt nanocube on a SiO₂ nanocube at 190 °C from ethylene, CO and H₂. Open squares = MeOH; open circles = propanal.

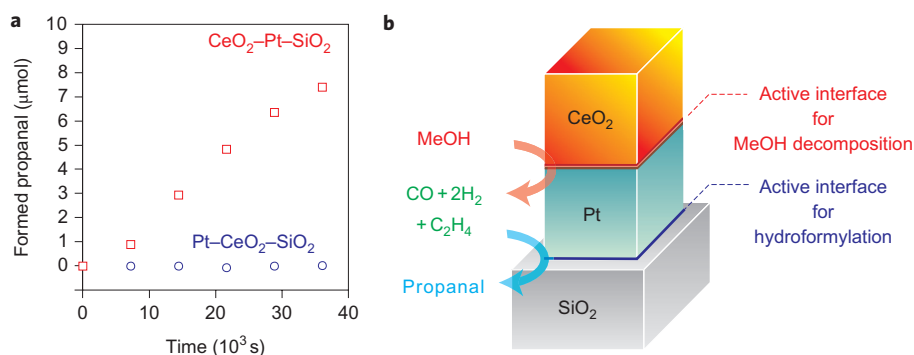


Figure 5 | Ethylene hydroformylation with MeOH over a tandem catalyst. **a**, Propanal produced as a function of reaction time over CeO₂-Pt-SiO₂ and Pt-CeO₂-SiO₂ bilayers at 190 °C from ethylene and MeOH. Open squares = CeO₂-Pt-SiO₂; open circles = Pt-CeO₂-SiO₂. **b**, Illustration of the CeO₂-Pt-SiO₂ tandem catalyst.

Hydroformylation with *in situ* decomposition of MeOH over the tandem CeO₂-Pt-SiO₂ catalyst gave a TOF for propanal of $2.6 \times 10^{-2} \text{ s}^{-1}$ per Pt atom, which was much faster than that obtained for ethylene hydroformylation with CO and H₂ gas over the Pt-SiO₂ catalyst. Two reasons for the better performance of the tandem catalyst are proposed here. First, for the *in situ* tandem catalytic reaction, MeOH decomposition occurred preferentially at the Pt-CeO₂ interface, but the rate of MeOH formation by CO hydrogenation decreased significantly because of the high MeOH concentration. The high density of CO and H₂ at the Pt surface is also beneficial for ethylene hydroformylation. Second, it is also possible that the electronic effects of CeO₂ contribute to change fundamentally the catalytic properties of the Pt-SiO₂ interface for more efficient hydroformylation.

To demonstrate the unique properties of our tandem catalysts, the same catalytic reactions were also examined over physical mixtures of Pt-CeO₂ and Pt-SiO₂ prepared by a conventional impregnation method. The Pt concentration was changed from 1 to 5 wt% for both catalysts. These physical mixture catalysts always produced ethane as a primary product and small amount of propane, which is likely to be formed by the successive hydrogenation of propanal (Supplementary Fig. S6). For a mixture of 3% Pt-SiO₂ and 3% Pt-CeO₂, the TOF of propane formation was $5.7 \times 10^{-4} \text{ s}^{-1}$ per Pt atom, which is much slower than the TOF of propanal formation, $2.6 \times 10^{-2} \text{ s}^{-1}$ per Pt atom, over the tandem catalyst. The different catalytic behaviours of the tandem catalyst and mixture catalysts clearly demonstrate the designed interfaces in our

tandem catalyst can be used to programme sequential chemical reactions effectively.

The novel concept of a nanocrystal bilayer ‘tandem catalyst’ involves multiple, distinct metal-metal oxide interfaces that correspond to specific catalytic activities and selectivities. This concept was tested using a CeO₂-Pt nanocube bilayer structure with well-defined surface structures on a silica substrate. Ethylene hydroformylation with H₂ and CO formed *in situ* by MeOH decomposition was demonstrated. Sequential chemical reactions at two different neighbouring metal-metal oxide interfaces acted to produce propanal selectively. Although tandem catalysis was employed previously in homogenous catalytic systems^{24,25}, this study is the first attempt to use rationally designed and assembled nanocrystal bilayers with multiple built-in metal-metal oxide interfaces. This new concept of nanocrystal tandem catalysis represents a powerful approach towards designing high-performance, multifunctional nanostructured catalysts for multiple-step chemical reactions, such as those proposed for artificial photosynthesis.

Methods

Synthesis of Pt and CeO₂ nanocubes. Pt nanocubes and CeO₂ nanocubes were prepared by reported methods with minor modifications^{19,20}. An aqueous solution of K₂PtCl₄ (10 mM, 1 ml) was added to an aqueous solution of TTAB (119 mM, 8.4 ml). After vigorous stirring, the solution was left at room temperature until a white crystalline solid formed. Then the mixture was heated at 50 °C with magnetic stirring until a clear solution was obtained. To the solution was added an ice-cold aqueous solution of NaBH₄ (500 mM, 0.6 ml). Excess H₂ that formed during the first 15 minutes was released through a needle. The solution was stirred for more than six

hours. The crude product was purified by discarding the precipitate following centrifugation at 3,000 r.p.m. (Precision Duraforce 200) for 30 minutes. The procedure was repeated four times. The shape of the particles was observed using a Tecnai 12 TEM or Tecnai G2 S-Twin.

Oleylamine-coated Pt nanocubes were obtained by performing ligand exchange on the purified Pt nanocubes described above. Pt nanocubes capped with TTAB were collected by centrifugation at 14,000 r.p.m. (VWR Galaxy 16D) for 30 minutes. The resulting powder (1.8×10^{-5} mol Pt, nominal) was then washed with deionized water twice and re-dispersed in water and oleylamine (61 μ mol, 20 μ l). The suspension was heated at 50 °C overnight with magnetic stirring. The slurry was then washed several times with MeOH and a chloroform/MeOH mixture before re-dispersing the particles in CHCl_3 .

CeO_2 nanocubes were prepared by autoclave at high temperature²⁰. Hydrochloric acid (50 μ l), toluene (15 ml), oleic acid (1.5 ml) and *tert*-butylamine (0.15 ml) were added to an aqueous solution of cerium nitrate hexahydrate (16.7 mM, 15 ml) in a Teflon cup (45 ml inner volume). The Teflon cup was sealed in a stainless-steel jacket and heated to 180 °C for 24 hours. The organic phase was collected and purified by centrifugation at 3,000 r.p.m. (Precision Duraforce 200) for five minutes. The particles were precipitated by the addition of double the volume of ethanol, followed by centrifugation at 14,000 r.p.m. (VWR Galaxy 16D) for ten minutes to isolate the yellowish white powder. The powder was washed twice with a hexane/ethanol mixture.

LB film preparation. Platinum LB films were prepared with oleylamine-capped Pt nanocubes. Following ligand exchange and washing, the Pt-oleylamine particles were re-dispersed in chloroform (0.5 ml). The solution was slowly dropped onto a water subphase on a LB trough. After evaporation of the chloroform for 30 minutes, the film was compressed until a surface pressure of 10–15 mN m⁻¹ was achieved. The resulting film was aged for 30 minutes and then transferred onto a Si substrate. CeO_2 nanocube LB films were prepared in the same manner with a chloroform solution of CeO_2 nanocubes. HRTEM images and EDX spectra were recorded on a Philips CM200.

Catalysis measurements. All catalysis measurements were carried out with a closed circulation set-up. A silicon wafer loaded with the nanocube bilayer film was put into a glass tube with an inner diameter of 11 mm. A stream of N_2 gas was passed over the sample, which was then heated to the desired temperature for measurement. The temperature was monitored with a thermocouple inserted into a glass sheath placed onto the sample. After the temperature stabilized, the reaction gas of 40 torr CO, 100 torr O_2 and 620 torr N_2 was introduced into the reaction chamber to examine the CO oxidation catalysis. The reaction products were quantified approximately every 30 minutes by gas chromatography with two columns and thermal conductivity detectors. A molecular sieve 5A column with Ar carrier gas was used to quantify O_2 , N_2 and CO, and a Poraplot Q column with He carrier gas was used for CO_2 quantification. The number of Pt atoms exposed to the reaction gas was estimated from scanning electron microscopy images. The MeOH decomposition reaction was carried out in a similar manner. N_2 gas with 30 torr MeOH was introduced into the reaction chamber with the catalyst. H_2 produced by the catalytic reaction was separated and quantified by the molecular sieve 5A column. Hydroformylation was performed with a gas mixture of 7.6 torr ethylene, 30 torr CO, 30 torr H_2 and 692 torr N_2 . The products were analysed every two hours. Propanal formed during the reaction was separated and quantified with a Poraplot Q column. Ethylene hydroformylation with H_2 and CO formed *in situ* by MeOH decomposition was investigated with a gas mixture of 7.6 torr ethylene, 30 torr MeOH and 722 torr N_2 . The estimation of TOF was based on the number of Pt atoms on the surface of the nanoparticles.

Received 10 September 2010; accepted 24 February 2011;
published online 10 April 2011

References

- Centi, G. & Perathoner, S. Catalysis: role and challenges for a sustainable energy. *Top. Catal.* **52**, 948–961 (2009).
- Norskov, J. K., Bligaard, T., Rossmeisl, J. & Christensen, C. H. Towards the computational design of solid catalysts. *Nat. Chem.* **1**, 37–46 (2009).
- Ott, L. S. & Finke, R. G. Transition-metal nanocluster stabilization for catalysis: a critical review of ranking methods and putative stabilizers. *Coord. Chem. Rev.* **251**, 1075–1100 (2007).
- Somorjai, G. A., Frei, H. & Park, J. Y. Advancing the frontiers in nanocatalysis, biointerfaces, and renewable energy conversion by innovations of surface techniques. *J. Am. Chem. Soc.* **131**, 16589–16605 (2009).
- Somorjai, G. A., Tao, F. & Park, J. Y. The nanoscience revolution: merging of colloid science, catalysis and nanoelectronics. *Top. Catal.* **47**, 1–14 (2008).
- Si, R. & Flytzani-Stephanopoulos, M. Shape and crystal-plane effects of nanoscale ceria on the activity of Au– CeO_2 catalysts for the water–gas shift reaction. *Angew. Chem. Int. Ed.* **47**, 2884–2887 (2008).

- Xie, X. W., Li, Y., Liu, Z. Q., Haruta, M. & Shen, W. J. Low-temperature oxidation of CO catalysed by Co_3O_4 nanorods. *Nature* **458**, 746–749 (2009).
- Stakheev, A. Y. & Kustov, L. M. Effects of the support on the morphology and electronic properties of supported metal clusters: modern concepts and progress in 1990s. *Appl. Catal. A* **188**, 3–35 (1999).
- Jackson, S. D. *et al.* Supported metal catalysts: preparation, characterization, and function. 5. Activities and selectivities of platinum catalysts in the reactions of cyclopropane, ethene, 1,3-butadiene, and 2-butyne with dihydrogen. *J. Catal.* **162**, 10–19 (1996).
- Jackson, S. D., Kelly, G. J. & Webb, G. Supported metal catalysts: preparation, characterization, and function – Part VI. Hydrogenolysis of ethane, propane, *n*-butane and *iso*-butane over supported platinum catalysts. *J. Catal.* **176**, 225–234 (1998).
- Zhou, Z., Kooi, S., Flytzani-Stephanopoulos, M. & Saltsburg, H. The role of the interface in CO oxidation on Au/ CeO_2 multi-layer nanotowers. *Adv. Funct. Mater.* **18**, 2801–2807 (2008).
- Shevchenko, E. V., Talapin, D. V., Kotov, N. A., O'Brien, S. & Murray, C. B. Structural diversity in binary nanoparticle superlattices. *Nature* **439**, 55–59 (2006).
- Urban, J. J., Talapin, D. V., Shevchenko, E. V., Kagan, C. R. & Murray, C. B. Synergism in binary nanocrystal superlattices leads to enhanced *p*-type conductivity in self-assembled PbTe/Ag₂Te thin films. *Nat. Mater.* **6**, 115–121 (2007).
- Aliaga, C. *et al.* Sum frequency generation and catalytic reaction studies of the removal of organic capping agents from Pt nanoparticles by UV–ozone treatment. *J. Phys. Chem. C* **113**, 6150–6155 (2009).
- Ungváry, F. in *Encyclopedia of Catalysis* Vol. 3 (ed. Horvath, I. T.) pp 734–787 (John Wiley, 2003).
- Croy, J. R. *et al.* Support dependence of MeOH decomposition over size-selected Pt nanoparticles. *Catal. Lett.* **119**, 209–216 (2007).
- Imamura, S. *et al.* Decomposition of methanol on Pt-loaded ceria. *Catal. Today* **50**, 369–380 (1999).
- Naito, S. & Tanimoto, M. Effect of sodium cation addition on the hydroformylation of propane over silica-supported Group VIII metal catalysts. *Chem. Commun.* 1403–1404 (1989).
- Lee, H. *et al.* Morphological control of catalytically active platinum nanocrystals. *Angew. Chem. Int. Ed.* **45**, 7824–7828 (2006).
- Yang, S. & Gao, L. Controlled synthesis and self-assembly of CeO_2 nanocubes. *J. Am. Chem. Soc.* **128**, 9330–9331 (2006).
- Contreras, A. M., Yan, X.-M., Kwon, S., Bokor, J. & Somorjai, G. A. Catalytic CO oxidation reaction studies on lithographically fabricated platinum nanowire arrays with different oxide supports. *Catal. Lett.* **111**, 5–13 (2006).
- Kweskin, S. J. *et al.* Carbon monoxide adsorption and oxidation on monolayer films of cubic platinum nanoparticles investigated by infrared–visible sum frequency generation vibrational spectroscopy. *J. Phys. Chem. B* **110**, 15920–15925 (2006).
- Panagiotopoulou, P. & Kondarides, D. I. A comparative study of the water–gas shift activity of Pt catalysts supported on single (MOx) and composite (MOx/Al₂O₃, MOx/TiO₂) metal oxide carriers. *Catal. Today* **127**, 319–329 (2007).
- Wasilke, J. C. *et al.* Concurrent tandem catalysis. *Chem. Rev.* **105**, 1001–1020 (2005).
- Felpin, F. X. & Fouquet, E. Heterogeneous multifunctional catalysts for tandem processes: an approach toward sustainability. *Chem. Sus. Chem.* **1**, 718–724 (2008).

Acknowledgements

This work was supported by the Director, Office of Basic Energy Sciences, Materials Sciences and Engineering Division, of the US Department of Energy under Contract No. DE-AC02-05CH11231.

Author contributions

Y.Y., C.T., G.S. and P.Y. conceived and designed the experiments. Y.Y., W.H. and C.A. performed the experiments. Z.H., S.H., T.S. and C.A. contributed materials and analysis tools. Y.Y., C.T., W.H. and P.Y. co-wrote the paper. All authors discussed the results and commented on the manuscript.

Additional information

The authors declare no competing financial interests. Supplementary information accompanies this paper at www.nature.com/naturechemistry. Reprints and permission information is available online at <http://npg.nature.com/reprintsandpermissions/>. Correspondence and requests for materials should be addressed to P.Y.